

Quercetin-loaded Solid Lipid Nanoparticles: Preparation and Characterization for Biomedical Application

Gamal Osman Elhassan¹, Jamal Moideen Muthu Mohamed^{2*}

¹ Department of Pharmaceutics, College of Pharmacy, Qassim University, Buriadah, Saudia Arabia

² Faculty of pharmacy & BioMedical Sciences, MAHSA University, Bandar Saujana Putra, 42610 Jenjarom, Selangor. Malaysia; jamalmoideen@mahsa.edu.my

Cite this paper as: Gamal Osman Elhassan, Jamal Moideen Muthu Mohamed (2024) Quercetin-loaded Solid Lipid Nanoparticles: Preparation and Characterization for Biomedical Application. *Frontiers in Health Informatics*, 13 (3), 680-686.

Abstract

In the proposed work, *quercetin (QuR)* loaded solid lipid nanoparticles (Q-SLNs) were prepared for biomedical applications using the nano-biomaterials of solid lipid, such as stearic acid (SA), and the surfactants tween 80 and span 80. The % drug loading and entrapment efficiency (EE (%)) for the optimized Q-SLN were 94.21 ± 6.44 % and 76.87 ± 8.2 %, respectively. There were strong relationships between the QuR incorporation and release patterns. Effective QuR delayed release was demonstrated by the results, which showed that over 63.45 ± 2.14 % of the bio-nano Q-SLNs was released gradually over the period of 60 h. Overall, the drug had been successfully loaded into the SLN, exhibiting a physicochemical compatibility without any chemical interaction with the used additives. According to the results, Q-SLN is the best vehicle for delivering QuR, and this preparation is utilized in a variety of treatments.

Keywords: Ultrasonication; Quercetin; Solid Lipid Nanoparticles, FTIR, in vitro drug release

1. Introduction

Breast cancer remains one of the most common malignancies affecting women globally, with significant implications for patient health and well-being. Despite advances in treatment, including surgery, chemotherapy, and radiation therapy, these interventions can be associated with substantial side effects and variable efficacy. Consequently, there is a growing interest in the potential of natural compounds, such as QuR, to complement existing therapies. Quercetin (QuR), a flavonoid found in many fruits and vegetables, has shown promise in preclinical studies for its anticancer properties. Solid lipid nanoparticles (SLNs) have been explored as a delivery system for QuR to enhance its bioavailability and therapeutic efficacy in breast cancer treatment [1].

The prevalence of breast cancer and the limitations of current treatments underscore the need for innovative therapeutic strategies. QuR, with its anti-inflammatory and antitumor activities, may improve the therapeutic outcomes when delivered effectively to the tumor site [2].

QuR anticancer effects are multifaceted, including the induction of apoptosis, inhibition of cell proliferation, and interference with angiogenesis. It modulates various signaling pathways, such as the PI3K/Akt and MAPK pathways, which are crucial in the regulation of cell growth and survival [3].

The bioavailability of QuR is limited due to poor solubility and extensive first-pass metabolism. SLNs have been developed to overcome these limitations, providing a means to enhance the solubility, stability, and bioavailability of QuR, as well as to facilitate targeted delivery to breast cancer cells (Martinez et al., 2023).

QuR SLNs are being investigated for their potential to serve as an adjunctive therapy in breast cancer management. Clinical trials are in progress to assess the efficacy and safety of QuR SLNs in patients with breast cancer, with some studies indicating improved outcomes [4].

QuR is generally recognized as safe when consumed in dietary amounts. However, the safety profile of QuR SLNs is still under investigation, and patients are advised to consult with healthcare providers before initiating any new treatment regimen [5].

In summary, QuR SLNs represent a novel approach to breast cancer therapy, with the potential to enhance the delivery and efficacy of QuR. Ongoing research is crucial to establish the clinical benefits and safety profile of QuR SLNs in the treatment of breast cancer [6].

2. Materials and Methods

2.1 Materials

We have purchased the following drugs from the Indian market. The free samples of stearic acid (SA) and **quercetin (QuR)** were obtained from SRL Pvt. Ltd. in Maharashtra, India. Sourced from Sigma Aldrich, Bangalore, India, Tween 80 and Span 80. In this investigation, analytical-grade chemicals and reagents were employed.

2.2. Formulation of QuR-loaded SLNs (Q-SLNs)

After the aqueous and oil phases were prepared independently, SLNs were formulated using the micro-emulsion method using QuR-loaded (Q-SLNs) and free SLN (blank SLN; B-SLN) [7]. Ultrasonication was then employed to finish the process, at first the aqueous phase consisted of nonionic surfactants such as span 80 and tween 80, whereas the oil phase consisted of QuR and SA. For 10 min, the two phases were heated concurrently to a distinct temperature of 70 °C. Following the addition of the oil phase, the aqueous phase was heated to 70 °C and exposed to sonication at different intervals. A heated ultrasonic bath (Tecno-GAZ SPA Ultra Sonic System) with a power rating of 120 W and a rate of 40 to 89 kHz was utilized. Following a 5 min stirring period, the emulsion was diluted with a final amount of 25 mL of cold water (2 to 4 °C). To achieve the required SLN, the suspension was next subjected to sonication using a sonicator at (Sonics & Materials VCX 750, Inc., Newtown, USA) for 15min (Amplitude 45%; pulse rate 9/3sec) for 15 min [8]. The resultant SLN were then kept at 4 °C after being lyophilized for 72 h for further analysis.

2.3. Compatibility study

To evaluate a potential interaction (difference in structure) between the QuR, SA and its physical mixture (PM), FT-IR analysis was conducted¹⁰. In a Fourier-transform infrared spectroscopy (FT-IR) spectrophotometer (JASCO/FT-IR-6300, Japan), the IR spectra of the solid samples was examined in the solid powder using the KBr disc method in the wavenumber range of 4000–400 cm⁻¹ at a scan speed of 1 cms⁻¹ [9].

2.4. Percentage entrapment efficiency (% EE)

The amount of integrated QuR (% EE) at 382 nm was measured using an Agilent Cary 60 UV-Vis Spectrophotometer (USA) after the aqueous dispersion had been run through a 0.45 m syringe filter. The quantity of additional QuR was calculated by subtracting the amount of original drug from the amount of free drug, after the determination of the amount of untrapped QuR in the filtrate [10]. To ascertain the drug percentage EE in the SLNs, equation (1) was utilized:

$$\% EE = \frac{\text{quantity of QuR added in Q - SLN} - \text{quantity of free QuR}}{\text{quantity of QuR added in Q - SLN}} \times 100 \quad \dots \dots \text{Eq. (1)}$$

2.5. *In vitro* release study

The optimal preparation of Q-SLNs was studied using the dialysis bag (M.W. cutoff: 12,000 Da) method, with a 50% ethanol and 50% phosphate buffer (50:50; PBS, pH 6.8) mixture used as the dissolution medium [11]. The dialysis bag was first filled with 10 mL of prepared Q-SLN after being immersed in PBS (pH 6.8) for a full day. After that, the dissolving medium was added, mixed, and kept at 37 ± 0.5 °C while being magnetically agitated at 100 rpm. After that, 2 mL of the dissolution medium was withdrawn and replaced at different intervals of time (0.5, 1, 2, 4, 8, 12, 24, 48, and 60 h hours) with the same amount of fresh dissolution medium (buffer). Spectrophotometry at 382 nm was used to measure the level of QuR in accordance with the stated methodology. Every test was conducted three times, and the results were shown as (mean \pm standard deviation).

2.6. Release Kinetics from Q-SLN

To comprehend the kinetics of drug release from the preparation, a number of kinetic release models were employed, such as the zero order (% CDR vs. time), the first order (% log of QuR balance vs. time), and the Higuchi model (% CDR vs. square root of time), Korsmeyer-Papas model and Hixon-crowell model [12]. The optimal performing and high linear (R^2) fitting model was identified using the highest regression values.

3. Results and Discussion

3.1. Determination of λ_{max}

The λ_{max} of CMN was determined first by scanning solution of CMN in a UV spectrophotometer and the λ_{max} was found to be 367 nm as shown in Figure 1a.

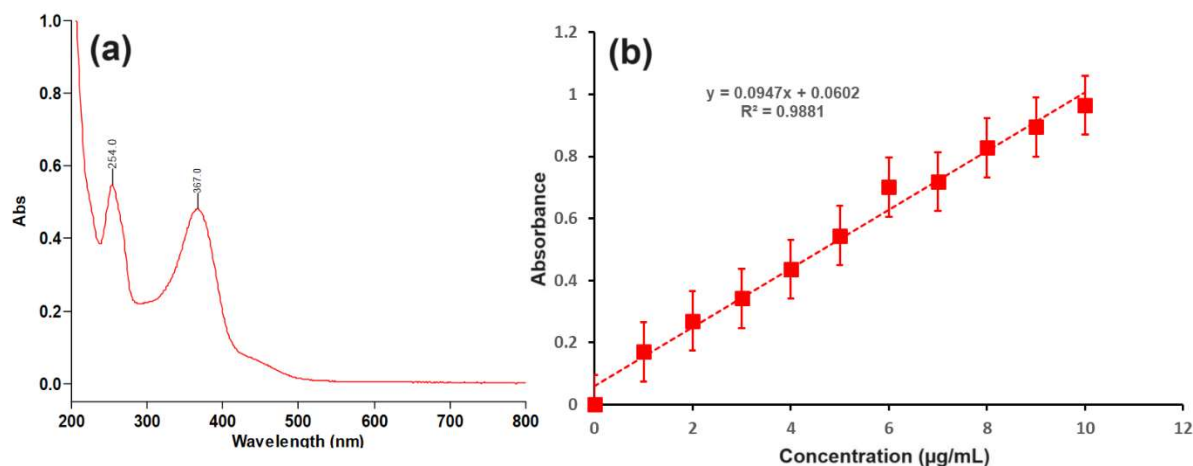


Figure 3. (a) UV Scan (at the concentration 9 µg/mL in the range of 200 to 800 nm) and (b) standard calibration curve of CMN

3.2. FTIR

FT-IR spectrum of samples and raw materials exhibited concern characteristic peaks shown in Figure 1. When determining the structure of a chemical, FT-IR spectroscopy can be used to track structural alterations and detect

the absorption peak of distinct functional groups. Literature [41] states that absorption bands 1600–1700, 1450–1550, and 1200–1450 cm^{-1} correspond to the N–H bending amide I band, C–N stretching amide II band, and N–H bending amide III band, respectively. For SPI here, absorption at 1649 cm^{-1} contributed to N–N bending in amide II and C=O stretching in amide I, as shown in Figure 1A; 1394 cm^{-1} is consistent with N–H bending and C–N stretching in the amide III band. According to carboxyl groups linked to the saturated aliphatic chain [13], SA exhibited weak O–H stretching at 3479 cm^{-1} , significant C–H stretching at 2914 and 2851 cm^{-1} , as well as at 1734 cm^{-1} (C=O stretching). These peaks demonstrate their high hydrophobic nature (Figure 2).

Comparative distinctive peaks from SA, QuR, for C–H vibrations, and C=O stretching from solid lipids and amide bands were shown by the Q-SLN components of all the spectra. Similarly, the coating changed the peak location and intensity of the amine groups at 668–911 cm^{-1} area caused by the twisting vibration, indicating the presence of N–H groups (PM). Because the carboxylate groups aided in the coating process, their strength (1385 cm^{-1}) in CP-SD-SLNs was diminished [14].

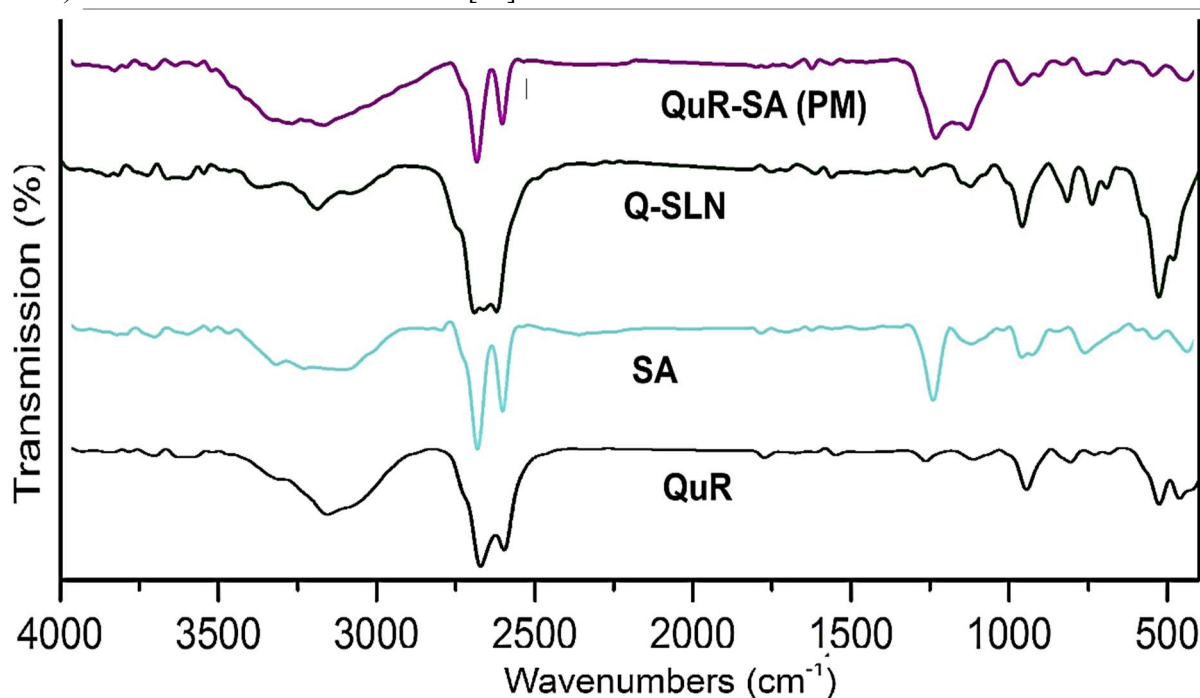


Figure 2. FTIR spectrum of (a) Free QuR, (b) SA, (c) QuR+SA (PM), and (d) Q-SLN.

In conclusion, the significant complexation of the QuR with the lipid and surfactant molecules is demonstrated by the decreased recurrence in the C=O stretching peak vibration corresponding to the drug. Because the drug was encapsulated in the lipid core, the peak corresponding to QuR was completely absent at C-SLNs and Q-SLNs, whereas the SA peak was present but at a lower intensity (2887 and 2812 cm^{-1} , respectively).

3.3. % EE and drug loading (%)

Because more particles in the aqueous and lipid phases interacted with one another and the drug left the lipid core, the percentage of EE decreased ($76.87 \pm 8.2\%$) as the sonication period was increased. Due to the lipophilic character of the QuR molecule that was trapped (drug loading) in the lipid matrix core ($94.21 \pm 6.44\%$), surfactant ratios have a substantial effect on the drug solubility in the superficial phase; nevertheless, the

effects were not observed to be particularly significant in this investigation [15]. Moideen et al. (2020) studied into the idea that the drug, which is very lipophilic, has a greater EE because it is more soluble in lipids. They found that when the concentration of lipids increased, the drug's EE in the SLNs increased as well, increasing the drug's partition in the exterior phase [16]. Numerous investigations revealed that while curcumin SLN was ideal (>80%), > 95% of EE was achieved because of the lipophilic drug present in the lipid core.

3.4. *In vitro* QuR release

This work used a dialysis bag to examine the *in vitro* release of QuR from SLNs during a 48-hour period at 37 ± 0.5 °C (Fig. 6a). QuR's poor water solubility meant that when 50% v/v of ethanol was added, the pH of the PBS was 6.8. According to our results, during the test period, 63.45 ± 2.14 % of the drug payload was released, which added to the 91.42 ± 8.71 % of free drug. Due to the slower diffusion of QuR through diffusion and dissolution mechanisms after the SLN inner solid matrix core, the release of SLNs was delayed and decreased after 12 h. Low viscosity or small molecular size prevail in the matrix, despite the complex circumstances that could affect their release rate, such as the SLNs large surface area and high diffusion coefficient [17].

The release characteristics of SLN and free QuR were assessed in this study. In addition, the release data was evaluated using the subsequent Higuchi equation: Where Q_t is the quantity of QuR released at time t and k is the release rate constant, $Q_t = kt^{0.5}$. The Higuchi model plot is used to compute the K values, or release rate constant, and the R^2 value of the *in vitro* release values indicates the release kinetics [18].

The linear fitting of the QuR release profile for homogeneous and granular matrix systems demonstrated its diffusion-controlled nature [38]. The Higuchi model has the highest R^2 value for QuR-SLNs, Fig. 6b shows, suggesting a typical diffusion-controlled drug release. The Higuchi model states that when a drug dissolves, diffuses out of the system, and the surrounding medium penetrates the matrix all at once, the drug is released from the matrix [19]. It is clear that the way the drugs were released from the SLNs was unaffected by lyophilization.

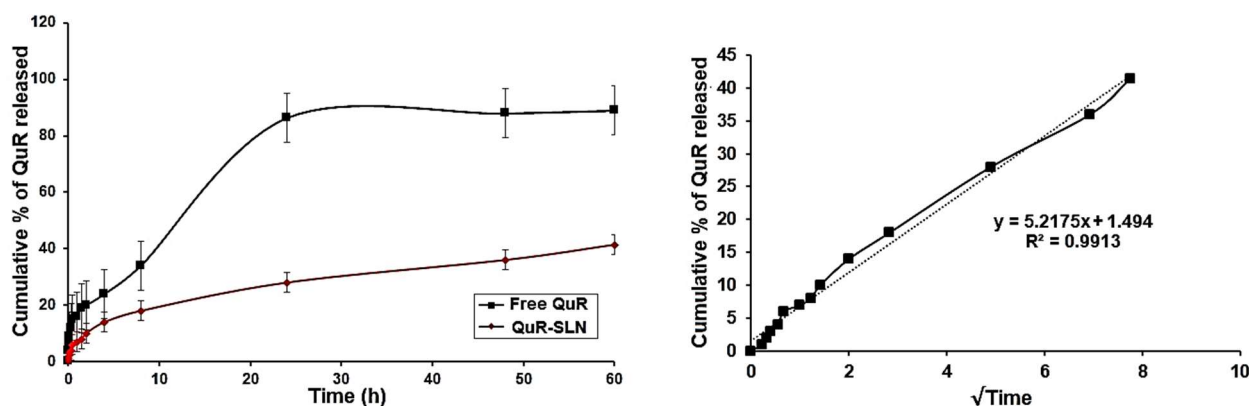


Figure 3. Cumulative % of QuR release from Q-SLN and (b) Higuchi model kinetic release of QuR-SLN (\sqrt{t} vs. time); (mean \pm SD, $n=3$)

4. Conclusion

This study successfully demonstrated the feasibility of formulating QuR-loaded solid lipid nanoparticles (SLNs)

as a promising approach for enhancing the bioavailability and therapeutic efficacy of QuR. The SLNs exhibited a favorable entrapment efficiency, and drug loading, indicating their potential for targeted delivery and sustained release. Characterization studies confirmed the successful encapsulation of QuR within the lipid matrix. In vitro release studies revealed a sustained release profile up to 60 h, suggesting the potential for prolonged drug exposure and reduced dosing frequency. Furthermore, the SLNs suggesting their potential for effective drug delivery to target tissues. Overall, the results of this study highlight the potential of QuR-loaded SLNs as a promising drug delivery system for various biomedical applications, particularly those requiring sustained release and enhanced bioavailability of QuR. Further in vivo studies are warranted to evaluate the safety, efficacy, and clinical translation of these nanoparticles.

Conflict of Interest

The authors have no conflicts of interest regarding this investigation.

Acknowledgment

I would like to thank to all staffs of Faculty of pharmacy & BioMedical Sciences, MAHSA University, Bandar Saujana Putra, 42610 Jenjarom, Selangor. Malaysia for helping for carrying this FYP research successfully.

References:

1. Lotfi N, Yousefi Z, Golabi M, Khalilian P, Ghezelbash B, Montazeri M, Shams MH, Baghbadorani PZ, Eskandari N. The potential anti-cancer effects of quercetin on blood, prostate and lung cancers: An update. *Front Immunol.* 2023;14:1077531. doi: 10.3389/fimmu.2023.1077531.
2. Michalkova R, Mirossay L, Kello M, Mojzisoava G, Baloghova J, Podracka A, Mojziz J. Anticancer Potential of Natural Chalcones: In Vitro and In Vivo Evidence. *Int J Mol Sci.* 2023;24(12):10354. doi: 10.3390/ijms241210354.
3. El-Hela AA, Bakr MSA, Hegazy MM, Dahab MA, Elmaaty AA, Ibrahim AE, El Deeb S, Abbass HS. *Sci. Pharm.* 2023;91:7.
4. Roy, H.; Panda, S. P.; Panda, S. K.; Tripathi, A. K.; Srivastava, S. K.; Nayak, B. S.; Singh, P. K.; Singh, G. D., N-trimethyl chitosan and tripalmitin loaded solid lipid nanoparticles of tofacitinib citrate: Characterization and in-vivo anti-inflammatory assessment. *Journal of Drug Delivery Science and Technology* 2023;87:104789.
5. Jacob S, Nair AB, Shah J, Gupta S, Boddu SH, Sreeharsha N, Joseph A, Shinu P, Morsy MA. *Pharmaceutics* 2022;14:533.
6. Muthu Mohamed JM, Kavitha K, Ahmad F, Sherbiny ME, Ebrahim D, El-Sagheer AM, Ebrahim HA, Abdelmonem Elsherbini DM, Ebrahim Abdelrahman MA, Dejene M. *Evid. Based Complement. Alternat. Med.* 2022:2022.
7. Ghasemiyeh P, Mohammadi-Samani S. Solid lipid nanoparticles and nanostructured lipid carriers as novel drug delivery systems: applications, advantages and disadvantages. *Res Pharm Sci.* 2018;13(4):288-303. doi: 10.4103/1735-5362.235156.
8. Gao W, Hu C-MJ, Fang RH, Zhang L. *Journal of Materials Chemistry B* 2013;1:6569-6585.
9. Kumar R, Singh A, Garg N, Siril PF. *Ultrason. Sonochem.* 2018;40:686-696.
10. Greenland S, Senn SJ, Rothman KJ, Carlin JB, Poole C, Goodman SN, Altman DG. *Eur. J. Epidemiol.*

2016;31:337-350.

11. Yadav K, Yadav D, Kumar S, Narra K, El-Sherbiny M, Al-Serwi RH, Othman G, Sendy JS, Mohamed JMM. Biomass Conversion and Biorefinery: 2022;1-13.
12. Satheesh V, Mohamed JMM, El-Sherbiny M, Othman G, Al-Serwi RH, Thilagar S. Biomass Conversion and Biorefinery. 2022;1-11.
13. Rahman N, Sameen S, Kashif M . J. Mol. Liq. 2019;274:270-277.
14. Mohamed JM, Alqahtani A, Ahmad F, Krishnaraju V, Kalpana . Carbohydr. Polym. 2021; 252:117180.
15. Mohamed JMM, Ahmad F, Alqahtani A, Raju VK, Anusuya M. Trends in Sciences 2021;18:1403-1403.
16. Moideen MMJ, Alqahtani A, Venkatesan K, Ahmad F, Krisharaju K, Gayasuddin M, Shaik RA. Application of the Box-Behnken design for the production of soluble curcumin: Skimmed milk powder inclusion complex for improving the treatment of colorectal cancer. Food Science & Nutrition. 2020;8(10):1-17, 2020; <https://doi.org/10.1002/fsn3.1957>
17. Maddiboyina, B.; Ramaiah; Nakkala, R. K.; Roy, H., Perspectives on cutting-edge nanoparticulate drug delivery technologies based on lipids and their applications. Chem. Biol. Drug Des. 2023;102(2):377-394.
18. Wang, Taoran & Ma, Xiaoyu & Lei, Yu & Luo, Yangchao. (2016). Solid lipid nanoparticles coated with cross-linked polymeric double layer for oral delivery of curcumin. Colloids and surfaces B: Biointerfaces. 2016;148:1-11. 10.1016/j.colsurfb.2016.08.047.
19. Jamal Moideen MM, Alqahtani A, Venkatesan K, Ahmad F, Krisharaju K, Gayasuddin M, Shaik RA, Ibraheem KMM, Salama MEdM, Abed SY. Food Science & Nutrition 2020;8:6643-6659.